ELSEVIER

Chemical Engineering Journal 137 (2008) 302–307

Chemical Engineering Journal

www.elsevier.com/locate/cej

Micro fluidized beds: Wall effect and operability

Xinhua Liu, Guangwen Xu *, Shiqiu Gao

State Key Laboratory of Multi-phase Complex System, Institute of Process Engineering, Chinese Academy of Sciences, Beijing 100080, PR China

Received 16 November 2006; received in revised form 14 April 2007; accepted 24 April 2007

Abstract

The minimum fluidization and minimum bubbling velocities of silica sand particles in air-blown micro beds of 120 mm high and with inner diameters of less than 32 mm were investigated to understand the wall effect in micro fluidized beds (MFBs) and the operability of the MFBs. Experimental results demonstrated that both the quoted velocities obviously increase with decreasing the inner diameter of the bed. A specific wall effect determined as the pressure drop per unit volume of particle bed in excess of the predicted pressure drop from the Ergun equation was proposed to quantitatively account for the influence of bed wall friction. By characterizing the fluidization qualities of differently sized particles in different MFBs, the article suggested further an optimal combination of bed diameter and particle size in the range of the static bed heights from 20 to 50 mm for the so-called micro fluidized bed (MFB) reactor devised to perform reaction(s) with minimal suffering from external gas mixing and gas diffusion.

Keywords: Wall effect; Gas–solid flow; Micro fluidized bed; Minimum fluidization velocity; Minimum bubbling velocity

1. Introduction

With more fluidized bed reactors being introduced into laboratory fundamental studies, miniaturization of fluidized beds is receiving increasing interest because a small-size bed has good operability and availability for some particularly required characteristics. The concept of micro fluidized beds (MFBs) was first put forward by Potic et al. [1] to refer to the beds with inner diameters of a few millimeters. What promotes the present study is accurate measurement of reaction kinetics of solid reactants, which is difficult to be performed in Thermal Gravimetric Analyzer (TGA). In TGA, a solid reactant has to be loaded into a sample cell before the chamber encasing the cell is heated. Thus, any reaction or physical variation of the reactant has to occur during heating, making TGA unable to measure accurately the reaction rate of the solid reactant at arbitrary temperatures. On the other hand, the reaction itself in the sample cell of a TGA may suffer seriously from external gas diffusion. But, a fluidized bed (FB) reactor may be free of the above-mentioned problems, which has thus been widely used to measure the rates of reactions such as pyrolysis, gasification, decomposition and so on. The FB reactor not only allows on-line feed of solid reactants at a preset temperature but diminishes also the gas-to-particle external diffusion with its flow turbulence, gas-particle shearing and particle-particle interaction. However, so far the employed FBs for studies of reaction kinetics generally have too large sizes, such as with an inner diameter above 50 mm and a bed height of a few hundreds of millimeters. This leads to serious gas mixing inside the reactor, causing the measured kinetic data based on changes of effluent gas composition to seriously deviate from real values. As a result, we are expecting to decrease this deviation to the utmost extent by replacing the fixed-bed reactor in TGA with a MFB reactor.

The fluidization characteristics (of a given kind of particles) in MFBs should be different from those in the ordinary-size fluidized beds due to much strong the wall effect in MFBs. From the viewpoint of operating and controlling a MFB kinetic analyzer, knowing the minimum fluidization and minimum bubbling velocities (U_{mf} and U_{mb}) enables us to determine the suitable gas velocities for the analyzer so that the fluidization in the MFB reactor can be maintained in its desirable state. Therefore, the present article is devoted to investigating U_{mf} and U_{mb} of silica sand particles in MFBs with inner diameters less than 32 mm and a bed height of 120 mm to throw more light on the

* Corresponding author at: State Key Laboratory of Multi-phase Complex System, Institute of Process Engineering, Chinese Academy of Sciences, P.O. Box 353, Beijing 100080, PR China. Tel.: +86 10 62550075; fax: +86 10 62550075.
E-mail address: gwxu@home.ipe.ac.cn (G. Xu).

1385-8947/$ – see front matter © 2007 Elsevier B.V. All rights reserved.
doi:10.1016/j.cej.2007.04.035

Nomenclature

A	cross-sectional area of the bed (m^2)
d_p	particle diameter (m)
D_t	bed diameter (m)
g	gravitational acceleration (m/s^2)
H_B	bed height (m)
H_s	static bed height (m)
m	mass of the particles in the bed (kg)
N	the number of samples
U_c	critical gas velocity (m/s)
U_g	superficial gas velocity (m/s)
U_{mb}	minimum bubbling velocity (m/s)
U_{mf}	minimum fluidization velocity (m/s)
V_B	volume of particle bed (m^3)
ΔP_0	pressure drop across the gas distributor (Pa)
ΔP_B	pressure drop across the particle bed (Pa)
ΔP_{Ergun}	pressure drop across the fixed bed (Pa)
ΔP_w	extra pressure drop resulting from the wall (Pa)
$\Delta \bar{P}_B$	averaged pressure drop across the bed (Pa)
ε	bed voidage
ρ_b	bulk density of the particles (kg/m^3)
ρ_g	density of the gas (kg/m^3)
ρ_s	real density of the particles (kg/m^3)
ϕ_s	shape factor of the particles
μ	viscosity of the gas (Pa s)
σ_P	standard deviation of pressure fluctuation at fluidization (Pa)

wall effect prevailing in the MFBs. By comparing the propensities to form gas channeling and particle slugging/plugging of differently sized particles in different MFBs under the operating conditions in this study, the article will find out further a suitable bed-particle combination for the use in MFB kinetic analyzers.

2. Experimental

2.1. Experimental set-up and procedure

A schematic diagram of experimental set-up is shown in Fig. 1. All experiments were carried out in three cylindrical quartz glass MFBs with a height of 120 mm and inner diameters (D_t) of 12, 20 and 32 mm, respectively. The top of every bed could be opened to accept particle load before experiment but was closed with a ground glass stopper in test. A sintered plate of 5 mm in thickness made from 150-μm silica sand particles was used as the MFB's gas distributor. As the outlet of the bed, there was a side tube of 10 mm i.d. on the top of every MFB, wherein another sintered plate was fixed with stuffed silica wool to prevent entrainment of fine particles with released gas. Air was used as the fluidizing gas and its flow rate was controlled with a mass flowmeter (GR116-1-A-PO&3, 5 LPM, Fathom Technologies, USA). The pressure drop across the bed was monitored with a differential pressure transducer (CP101/102PO&500, 1000, 2000 Pa, KIMO Instruments, France). All data were recorded

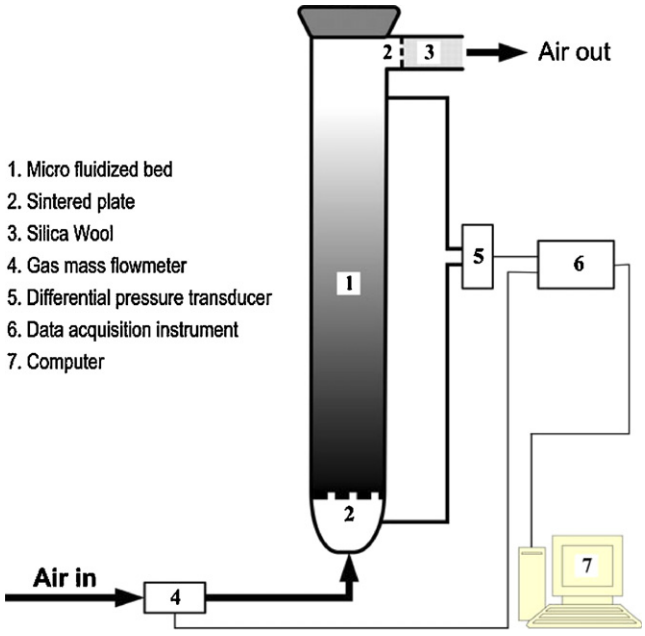

Fig. 1. Experimental set-up.

on a data acquisition instrument at a given sampling frequency and then transferred to a computer.

In order to examine the effect of particle sizes on fluidization behavior, three kinds of differently sized silica sand particles characterized in Fig. 2 were chosen as the fluidizing material. The pressure drops ΔP_0 across the distributor of each MFB at various superficial gas velocities measured in empty beds were shown in Fig. 3. By subtracting ΔP_0 from the total pressure drop across the fluidized bed, one can determine the pressure drop ΔP_B across the particle bed. The sampling frequency was 100 Hz for all pressure signals and more than 10,000 points were taken in every measurement. In the course of all experiments, the superficial gas velocity U_g was first gradually increased at small intervals until the silica sand particles were fully fluidized. Then, the experiments continued by decreasing U_g back to zero. Three static bed heights, $H_s = 20$, 35 and 50 mm, were investigated in three different MFBs, respectively. Both the total pressure drop and the bed height H_B were recorded as a function of U_g during all experiments.

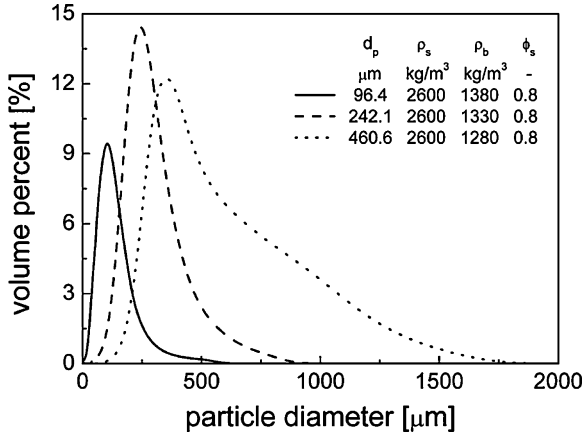

Fig. 2. Differential size distributions of three kinds of silica sand particles tested.

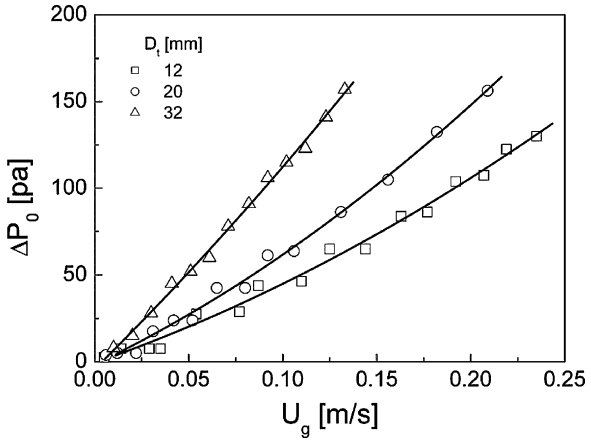

Fig. 3. Pressure drops across the distributor of each MFB at various superficial gas velocities.

2.2. Treatment of experimental data

The minimum fluidization velocity U_{mf} was generally defined as the gas velocity corresponding to the intersection of the pressure drop line for fixed bed with the horizontal line for fully fluidized bed. Loezos et al. [2] noted that some extra cohesive force between particles need to be overcome when increasing U_g to fluidize particles, which makes the measured U_{mf} much more unstable in U_g-ascending run than U_g-descending run [3]. Therefore, as exemplified by curve a in Fig. 4, we determined U_{mf} in U_g-descending run according to the Richardson's classic method [4].

The minimum bubbling velocity U_{mb} was determined generally by visually catching the first bubble appearing on the surface of the bed. However, the method is rather subjective, even infeasible in some cases. This is just the encounter of our tests. On the other hand, we found that the standard deviation σ_P of pressure fluctuation estimated from

$$\sigma_P = \left[\frac{1}{n-1}\sum_{i=1}^{n}(\Delta P_{Bi} - \Delta \bar{P}_B)\right]^{0.5} \quad (1)$$

evidently increases with the formation of obvious bubbles (see curve b in Fig. 4). Thus, in this study U_{mb} was defined from the point whereat σ_P starts to increase continuously and quickly with increasing U_g. The definition implicates that stable bubbles smaller than the bed size would form continuously when U_g is beyond U_{mb}. From Fig. 4, it can be seen that the experimental U_{mb} is lower than the experimental U_{mf}. This may be explained by the fact that the sand particle of 460.6 μm belonging to group B according to the Geldart classification was used as the fluidizing material in the experimental run, which leaded to the formation of the bubbles even before the minimum fluidization point since U_{mb} depends primarily on particle sizes but U_{mf} varies approximately with the square of particle sizes [5].

When U_g increases from zero to a critical value U_c (less than U_{mb}), the pressure drop ΔP_B across the particle bed may approach its maximum and becomes even greater than the weight of fluidized particles in the bed of unit cross-sectional area (see curve c in Fig. 4). Loezos et al. [2] found that this overpressure in gas–solid fluidization can be attributed primarily to the wall effect and the extent of overshoot pressure drop generally decreases with increasing bed sizes. Since the gas–solid system is still a fixed bed in the range of $0 < U_g \leq U_c$, its inherent pressure drop should be subject to the gas-particle friction calculated from the

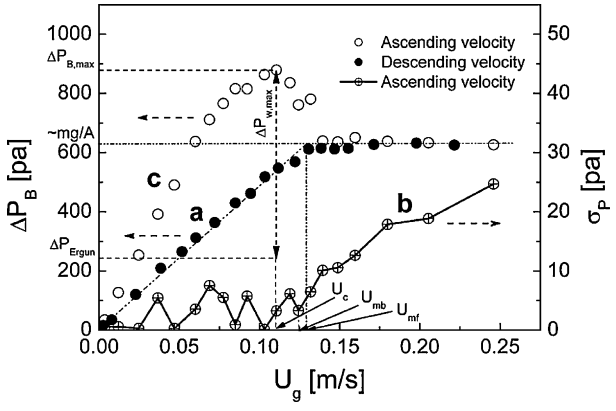

Fig. 4. Determination of U_{mf}, U_{mb} and ΔP_W in a typical operation (D_t = 12 mm, d_p = 460.6 μm and H_s = 50 mm).

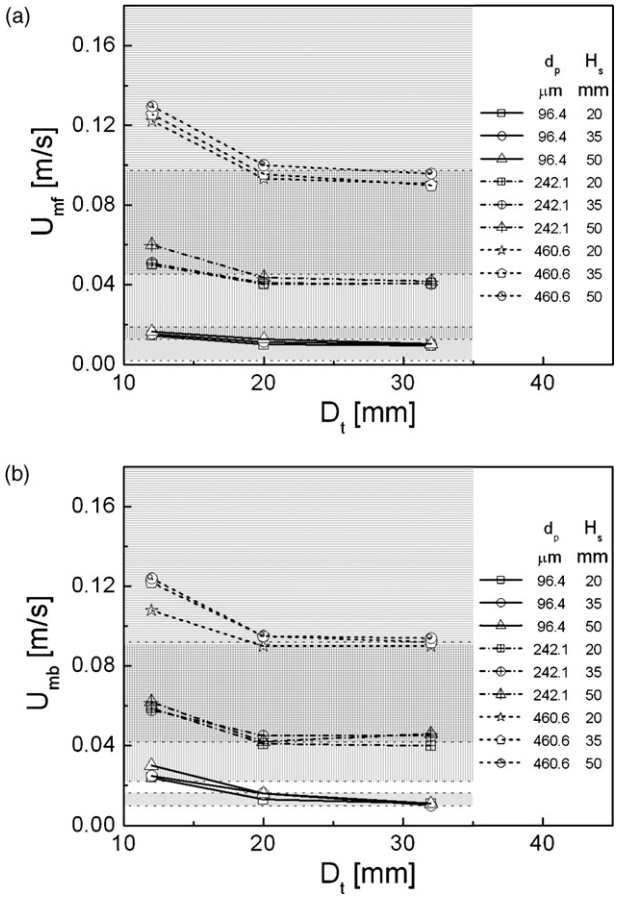

Fig. 5. Variations of (a) U_{mf} and (b) U_{mb} with D_t under different conditions (The shadow areas show the variation ranges of predicted U_{mf} and U_{mb} from literature correlations. The upper limits of the ranges for d_p = 460.6 μm are too large to show in the plot: ▨ d_p = 96.4 μm; ▥ d_p = 242.1 μm; ▤ d_p = 460.6 μm).

Ergun equation,

$$\frac{\Delta P_{\mathrm{Ergun}}}{H_{\mathrm{B}}} = 150\frac{(1-\varepsilon)^2}{\varepsilon^3}\frac{\mu U_{\mathrm{g}}}{(\phi_{\mathrm{s}} d_{\mathrm{p}})^2} + 1.75\frac{1-\varepsilon}{\varepsilon^3}\frac{\rho_{\mathrm{g}} U_{\mathrm{g}}^2}{\phi_{\mathrm{s}} d_{\mathrm{p}}}. \quad (2)$$

The actually measured pressure drop ΔP_{B} at a given U_{g}, on the other hand, is generally higher than $\Delta P_{\mathrm{Ergun}}$. Hence, an extra pressure drop per unit volume of particle bed determined as

$$\frac{\Delta P_{\mathrm{w}}}{V_{\mathrm{B}}} = \frac{\Delta P_{\mathrm{B}} - \Delta P_{\mathrm{Ergun}}}{\pi D_{\mathrm{t}}^2 H_{\mathrm{B}}/4} = \frac{\Delta P_{\mathrm{B}}/H_{\mathrm{B}} - \Delta P_{\mathrm{Ergun}}/H_{\mathrm{B}}}{\pi D_{\mathrm{t}}^2/4} \quad (3)$$

can be used to quantify the specific strength of bed wall friction. In Eq. (2), the parameter ε refers to the average bed voidage calculated from

$$\varepsilon = 1 - \frac{H_{\mathrm{s}}\rho_{\mathrm{b}}}{H_{\mathrm{B}}\rho_{\mathrm{s}}} \quad (4)$$

3. Results and discussion

Fig. 5(a and b) shows the variations of U_{mf} and U_{mb} with D_{t} under all the tested conditions, respectively. Comparing these two figures demonstrates that for given D_{t} and H_{s} the experimental U_{mb} is generally greater than the experimental U_{mf} at $d_{\mathrm{p}} = 96.4\,\mu\mathrm{m}$ (Geldart A), but becomes very close to U_{mf} at $d_{\mathrm{p}} = 242.1\,\mu\mathrm{m}$ (Geldart B) and even less than U_{mf} at $d_{\mathrm{p}} = 460.6\,\mu\mathrm{m}$ (Geldart B). Many literature works have shown that U_{mb} is generally larger than U_{mf} for group A particles, but may be smaller than U_{mf} for group B particles [5,6]. The results clarified in Fig. 5 comply with the literature observation, indicating in fact that the adopted definition of U_{mb} in this study is rational because the determination of U_{mf} involves rather a standard approach to make U_{mf} highly confident in all cases.

It can also be seen from Fig. 5 that static bed height H_{s}, as suggested by Broadhurst and Becker [7], has no observable effects on both U_{mf} and U_{mb} for all the tested d_{p} and MFBs. Both U_{mf} and U_{mb} decrease obviously with decreasing d_{p} and increasing D_{t}, but the decreasing degree of U_{mf} and U_{mb} with increasing D_{t} tends to decrease, even disappears when the bed diameter is large enough, for example, at $D_{\mathrm{t}} > 20\,\mathrm{mm}$ for Fig. 5. A number of existing empirical correlations were selected to predict the U_{mf} [7–20] and U_{mb} [7,21–22] of the tested systems. The shadow areas in Fig. 5(a and b) show the variation ranges of the resulting U_{mf} and U_{mb}, respectively. Most of the experimental measurements fall in the ranges of the predicted values, but the experimental values from $D_{\mathrm{t}} = 12\,\mathrm{mm}$ exceed the upper limit of the predictions. Hence, the existing literature correlations for U_{mf} and U_{mb} are probably applicable to the beds with inner diameters over 20 mm, but they evidently underestimate both the parameters in rather smaller beds. The implied essence is that the literature correlations, which were from larger beds, are unable to reproduce the wall effect prevailing in the beds with inner diameters below 20 mm.

Loezos et al. [2] suggested that the extent of pressure drop overshoot determined as $(\Delta P_{\mathrm{B}} A/mg - 1)$ quantitatively represents the strength of the wall effect. However, the physical meaning of $(\Delta P_{\mathrm{B}} A/mg - 1)$ is somewhat ambiguous because the

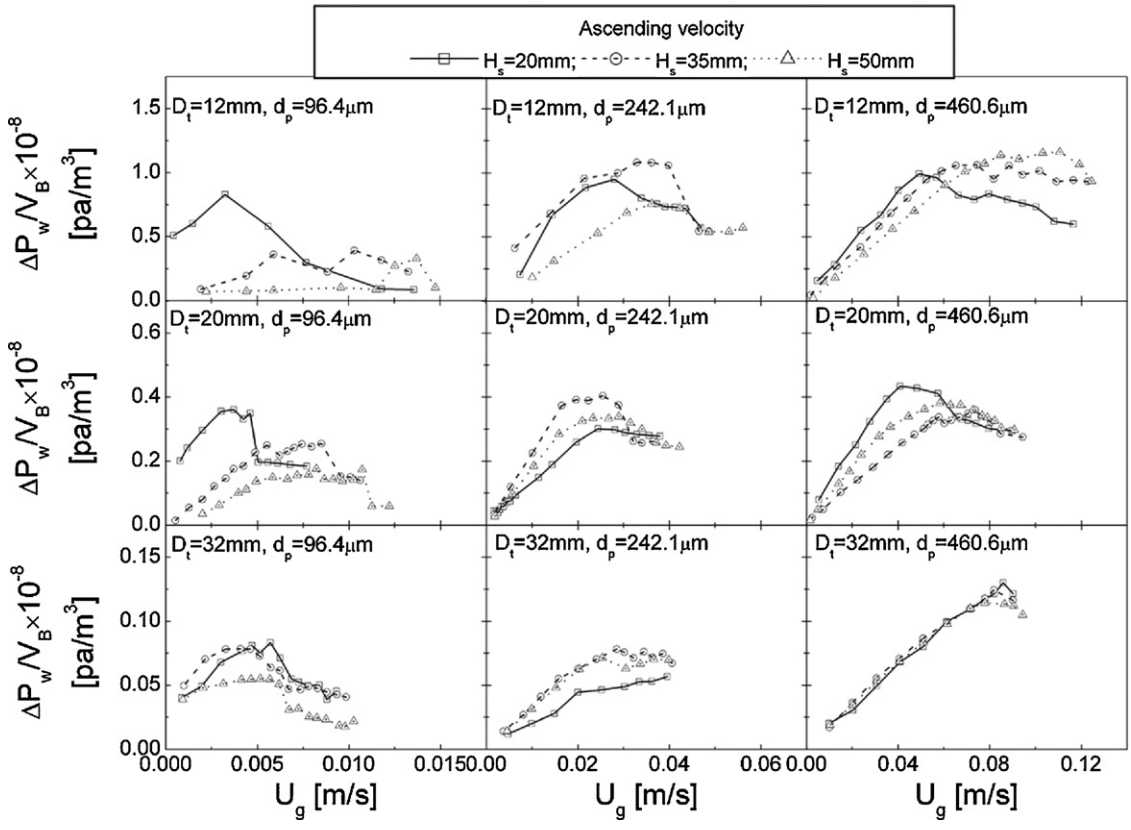

Fig. 6. Variations of $\Delta P_{\mathrm{w}}/V_{\mathrm{B}}$ with U_{g} under different H_{s}, D_{t} and d_{p}.

pressure drop overshoot occurs before the particles in the bed are completely fluidized, whereas the real pressure drop without wall effect is not mg/A but is subject to the friction estimated with, for example, the Ergun equation. Following this concern, we thus defined the parameter $\Delta P_w/V_B$ shown in Eq. (3). As shown in Fig. 6, this parameter varies with U_g under the condition of $U_g < U_{mf}$, and at $U_g = U_c$ it reaches a maximum estimated as

$$\frac{\Delta P_{w,max}}{V_B} = \frac{(\Delta P_B/H_B - \Delta P_{Ergun}/H_B)_{U_g=U_c}}{\pi D_t^2/4}. \quad (5)$$

Noting that $\Delta P_{w,max}/V_B$ represents the maximum extra pressure drop per unit volume of particle bed induced by the bed wall, we think that this newly defined parameter could provide an alternatively new measure to the wall-effect-induced extra barrier that should be overcome for the particles to be fully fluidized in a bed. Fig. 7 reveals that $\Delta P_{w,max}/V_B$ decreases with increasing D_t under all tested operating conditions, but may be anticipated to vary little with d_p and H_s when the inner diameter of the MFB is greater than 20 mm. The result reasonably accounts for the decrease of U_{mf} with increasing D_t and the little effect of H_s on U_{mf} clarified in Fig. 5(a). But in the MFBs with inner diameters below 20 mm, the maximum extra pressure drop $\Delta P_{w,max}$ may increase with increasing both d_p and H_s because large particles and great static bed heights lead to much serious slugging and more stronger particle-wall interaction. Therefore,

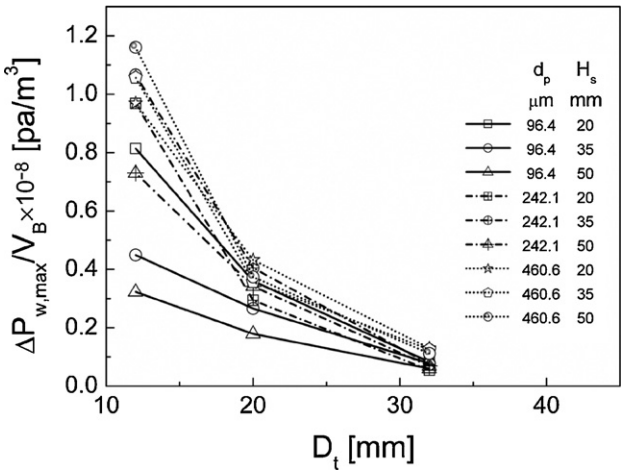

Fig. 7. Variations of $\Delta P_{w,max}/V_B$ with D_t under different H_s and d_p.

as shown in Fig. 7, in the MFB of i.d. = 12 mm an increase of d_p generally results in increasing $\Delta P_{w,max}/V_B$, but the effect of H_s on $\Delta P_{w,max}/V_B$ is not obvious due to the proportional variation of V_B with H_s.

Fig. 8 reproduces the standard deviation σ_P of pressure signals measured across all the tested MFBs. The deviation σ_P generally increases with increasing d_p and H_s and is lower for larger D_t under a given U_g. Meanwhile, the degree that σ_P

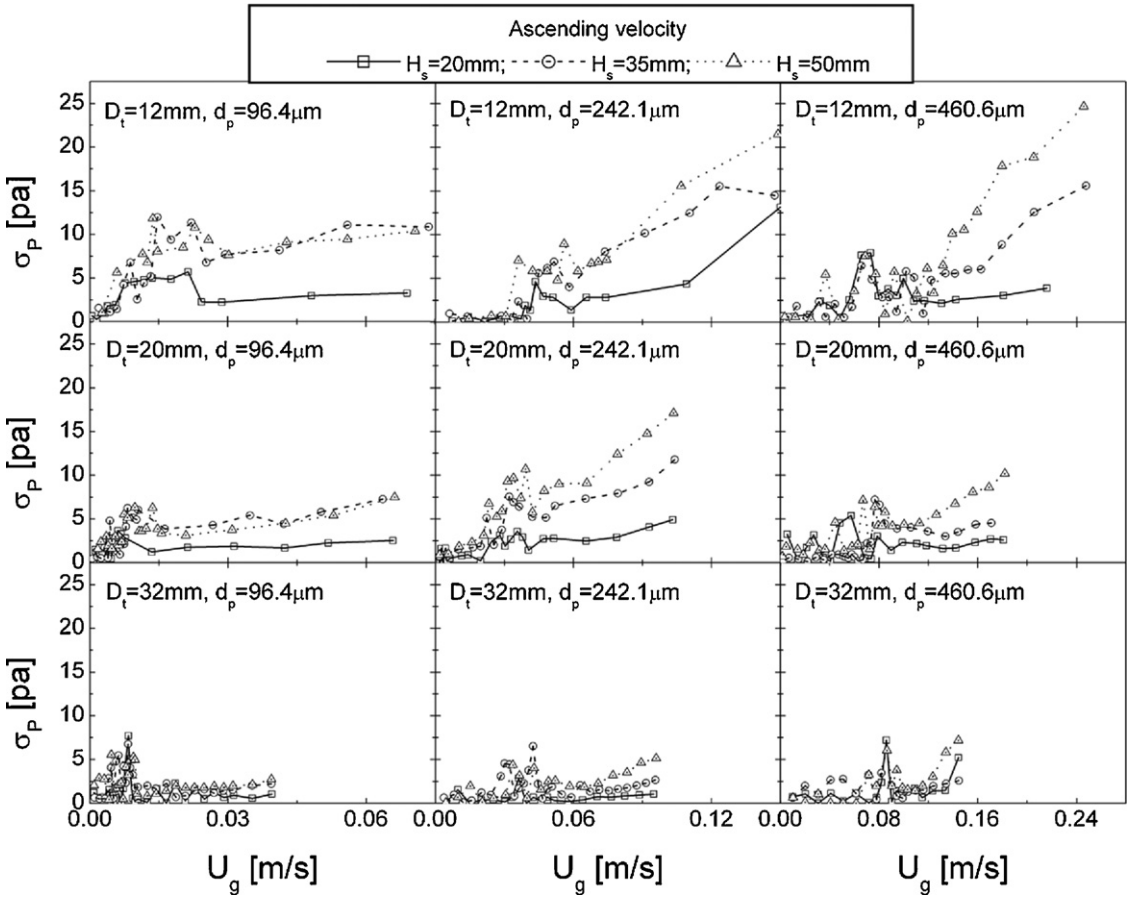

Fig. 8. Variations of σ_P with U_g at U_g-ascending tests under different conditions.

increases with increasing U_g is higher for smaller D_t and larger d_p. All of these features justify the variations of bubbling characteristics with bed diameters and particle sizes. That is, the larger particles likely lead to larger bubbles, while the bubbling flow in a smaller bed tends to present as the slugging/plugging type. Therefore, the minimum bubbling velocity U_{mb} tends to increase with increasing d_p and decreasing D_t, as shown in Fig. 5(b). In fact, the experiments also showed that slugging fluidization occurs obviously in the MFB of i.d. = 12 mm under the operating conditions, whereas gas channeling may happen in the bed of i.d. = 32 mm when U_g ranges from zero to about $1.5U_{mf}$. As shown in Fig. 3, the pressure drop ΔP_0 of the gas distributor in the MFB of i.d. = 32 mm is much greater than that in the other two smaller MFBs for the same U_g. That is, there should not exist nonuniform distribution of the gas flow in the MFB of i.d. = 32 mm since the same particles can be fluidized homogeneously and stably in the MFB of i.d. = 20 mm under the same operating conditions. So, the gas channeling occurring in the MFB of i.d. = 32 mm may be attributed to a relative low U_g in this study. Just because of this gas channeling, in Fig. 8 σ_P is higher for fixed bed than for fluidized bed in the case of i.d. = 32 mm (third row). Certainly, neither slugging fluidization nor gas channeling is favorable to the bed intended to be employed as a fluidized bed reactor. In the view of selecting a suitable bed–particle combination for the use as a micro fluidized bed reactor, we hence suggest that the MFB of i.d. = 20 mm with silica sand particles of d_p = 242.1 μm in the range of the static bed heights from 20 to 50 mm should be the best choice due to stable and homogeneous fluidization for this system.

4. Conclusions

- In micro fluidized beds (MFBs) with inner diameters of 10–32 mm the minimum fluidization velocity can be determined with the same method used ever for the other large-size beds, but the determination of the minimum bubbling velocity through the usually adopted visual observation of the appearance of the first gas bubble is rather difficult.
- The minimum fluidization and minimum bubbling velocities both exhibited an evident decrease when increasing the bed diameter from 12 to 20 mm. Above 20 mm the bed diameter only slightly affected such two velocities. Consequently, the article suggested that the bed wall effect may be extremely significant in the 12 mm bed.
- Through defining and calculating the extra pressure drop per unit bed volume in excess of that calculated from the Ergun equation, the bed wall effect in MFBs was found to decrease with increasing the bed diameter, but has little relation with both particle size and static bed height when the bed diameter is greater than 20 mm.
- A bed of an i.d. of about 20 mm was suggested to be suitable for the silica sand particles of 242.1 μm in the range of the static bed heights from 20 to 50 mm to make the bed relatively stably and homogeneously fluidized to be eligible for a MFB reactor. The MFB reactor is believed effective for suppressing external gas mixing and diffusion to make it suitable for reaction kinetics measurement.

References

[1] B. Potic, S.R.A. Kerstn, M. Ye, M.A. van der Hoef, J.A.M. Kuipers, W.P.M. van Swaaij, Fluidization with hot compressed water in micro-reactors, Chem. Eng. Sci. 60 (2005) 5982–5990.

[2] P.N. Loezos, P. Costamagna, S. Sundaresan, The role of contact stresses and wall friction on fluidization, Chem. Eng. Sci. 57 (2002) 5123–5141.

[3] C.L. Lin, M.Y. Wey, S.D. You, The effect of particle size distribution on minimum fluidization velocity at high temperature, Powder Technol. 126 (2002) 297–301.

[4] J.F. Richardson, Incipient fluidization and particulate systems, in: J.F. Davidson, D. Harrison (Eds.), Fluidization, Academic Press, London, 1971, pp. 25–64.

[5] D. Geldart, Types of gas fluidization, Powder Technol. 7 (5) (1973) 285–292.

[6] S. Simone, P. Harriott, Fluidization of fine powders with air in the particulate and the bubbling regions, Powder Technol. 26 (1980) 161–167.

[7] T.E. Broadhurst, H.A. Becker, Onset of fluidization and slugging in beds of uniform particles, AIChE J. 21 (1975) 238–247.

[8] M. Leva, Fluidization, McGraw-Hill, New York, 1959.

[9] C.Y. Wen, Y.H. Yu, A generalized method for predicting the minimum fluidization velocity, AIChE J. 12 (1966) 610–612.

[10] P. Bourgeois, P. Grenier, The ratio of terminal velocity to minimum fluidizing velocity for spherical particles, Can. J. Chem. Eng. 46 (1968) 325–328.

[11] B.C. Pillai, M. Raja Rao, Pressure drop & minimum fluidization velocities in air-fluidized beds, Indian J. Technol. 9 (3) (1971) 77–86.

[12] S.P. Babu, B. Shah, A. Talwalkar, Fluidization correlation for coal gasification materials - minimum fluidization velocity and fluidized bed expansion ratio, AIChE Symp. Ser. 176 (1978) 176–186.

[13] J.F. Richardson, M.A. Jeronimo, Velocity-voidage relations for sedimentation and fluidization, Chem. Eng. Sci. 34 (1979) 1419–1422.

[14] K. Doichev, N.S. Akhmakov, Fluidization of polydisperse systems, Chem. Eng. Sci. 34 (1979) 1357–1359.

[15] A. Lucas, J. Arnaldos, J. Casal, L. Puigjaner, High temperature incipient fluidization in mono and polydisperse systems, Chem. Eng. Commun. 41 (1986) 121–132.

[16] J.V. Fetcher, M.D. Deo, F.V. Hanson, Re-examination of minimum fluidization velocity correlations applied to group B sands and coked sands, Powder Technol. 69 (1992) 147–155.

[17] B.C. Lippens, J. Mulder, Prediction of the minimum fluidization velocity, Powder Technol. 75 (1993) 67–78.

[18] A.K. Bin, Prediction of the minimum fluidization velocity, Powder Technol. 81 (1994) 197–199.

[19] A. Barbosa, D. Steinmetz, H. Angelino, Heat transfer around spherical probes in bubbling fluidized beds, in: J. Large, C. Laguerie (Eds.), Fluidization VIII, vol. 1, 1995, pp. 145–152.

[20] R. Coltters, A.L. Rivas, Minimum fluidization velocity correlations in particulate systems, Powder Technol. 147 (2004) 34–48.

[21] A.R. Abrahamsen, D. Geldart, Behaviour of gas-fluidized beds of fine powders, part II. Voidage of the dense phase in bubbling beds, Powder Technol. 26 (1980) 47–55.

[22] M. Sciazko, J. Bandrowski, Effect of pressure on the minimum bubbling velocity of polydisperse materials, Chem. Eng. Sci. 40 (10) (1985) 1861–1869.